nature materials

ARTICLES

PUBLISHED ONLINE: 24 MARCH 2013 | DOI: 10.1038/NMAT3595

A molecular design principle of lyotropic liquid-crystalline conjugated polymers with directed alignment capability for plastic electronics

Bong-Gi Kim[1], Eun Jeong Jeong[2], Jong Won Chung[3], Sungbaek Seo[1], Bonwon Koo[3] and Jinsang Kim[1,2,4]*

Conjugated polymers with a one-dimensional *p*-orbital overlap exhibit optoelectronic anisotropy. Their unique anisotropic properties can be fully realized in device applications only when the conjugated chains are aligned. Here, we report a molecular design principle of conjugated polymers to achieve concentration-regulated chain planarization, self-assembly, liquid-crystal-like good mobility and non-interdigitated side chains. As a consequence of these intra- and intermolecular attributes, chain alignment along an applied flow field occurs. This liquid-crystalline conjugated polymer was realized by incorporating intramolecular sulphur–fluorine interactions and bulky side chains linked to a tetrahedral carbon having a large form factor. By optimizing the polymer concentration and the flow field, we could achieve a high dichroic ratio of 16.67 in emission from conducting conjugated polymer films. Two-dimensional grazing-incidence X-ray diffraction was performed to analyse a well-defined conjugated polymer alignment. Thin-film transistors built on highly aligned conjugated polymer films showed more than three orders of magnitude faster carrier mobility along the conjugated polymer alignment direction than the perpendicular direction.

Conjugated polymers (CPs) are active materials for various optoelectronic applications, such as organic solar cells, thin-film transistors, light-emitting diodes, and optical and amperometric sensors[1–10]. Their optical and electronic properties, such as absorption, emission and conductivity, are highly anisotropic owing to the one-dimensional (1D) *p*-orbital overlap along the conjugated polymer backbone. In consequence, unless conjugated polymers are molecularly and macroscopically assembled and aligned with a well-defined structure, their interesting properties cannot be fully realized in their device applications. A commonly used and effective method to create macroscopic alignment is to uniformly expose a rigid body having a high aspect ratio to a flow field, just as molecular liquid crystals preferentially orient to an applied shear force[11–13]. Secondary interactions, such as aromatic π–π interaction, intramolecular chalcogen–chalcogen interaction and hydrogen bonding, have been proposed as a promising tool to modulate CPs' self-assembly and possible alignment when they are rationally incorporated into a molecular design[1,14–16]. In reality, however, the directed assembly and particularly macroscopic alignment of CPs is a challenging task. In solution, CPs usually do not have a planar structure as a consequence of the low rotational energy barrier along the conjugated backbone. Therefore, in spite of their rigid rod-like molecular structure, CPs do not have good self-organization unless they are concentrated. Individual polymer chains in a solution cannot be aligned along a flow field probably owing to their small size and tumbling. However, in a condensed solution CPs aggregate and once CPs form crystalline domains, the reduced aspect ratio and low mobility of the crystallized domain will make CP alignment along an external flow field unfavourable. Nevertheless, there have been efforts to align conjugated polymers by applying an external force. The Langmuir–Blodgett film transfer method was used to align rod-like CPs (refs 17,18). However, the alignment of the CP by this method was mediocre, which is probably due to the formation of large-size assembled CP domains at the air/water interface and the relatively weak driving force. By this method, a dichroic ratio of 5.0–6.3 was obtained; that is, the absorption intensity parallel to the alignment direction was 5.0–6.3 times larger than that perpendicular to the alignment direction. Uniaxial tensile drawing of a CP within an ultrahigh-molecular-weight polyethylene matrix was also successfully implemented to achieve a much higher dichroic ratio of 15 in absorption and 20 in emission, respectively[19,20]. However, the application of the highly oriented CPs achieved by this method is limited to polarized photoluminescence because the CPs are embedded in the insulating polyethylene matrix. Dip coating of CPs on a substrate was also investigated as an aligning method[21]. The dichroic ratio was not directly investigated but the hole mobility of the resulting film along the dipping direction was measured to be two to three times faster than that perpendicular to the dipping direction. Nanoimprinting was also applied to two different CPs to achieve alignment by means of nanoconfinement[22]. The thermotropic liquid-crystalline CP showed a dichroic ratio of 12 in emission but the other CP did not show any alignment. The authors concluded that the lack of packing prevented CP assembly and alignment but did not investigate the detailed molecular design requirements. Even though these methods provide a certain degree of CP alignment, to fully

[1]Macromolecular Science and Engineering, University of Michigan, Ann Arbor, Michigan 48109, USA, [2]Department of Materials Science and Engineering, University of Michigan, Ann Arbor, Michigan 48109, USA, [3]Display Device Laboratory, Materials and Device Institute, Samsung Advanced Institute of Technology, Samsung Electronics Company, Youngin 446-712, Korea, [4]Department of Chemical Engineering, University of Michigan, Ann Arbor, Michigan 48109, USA. *e-mail: jinsang@umich.edu

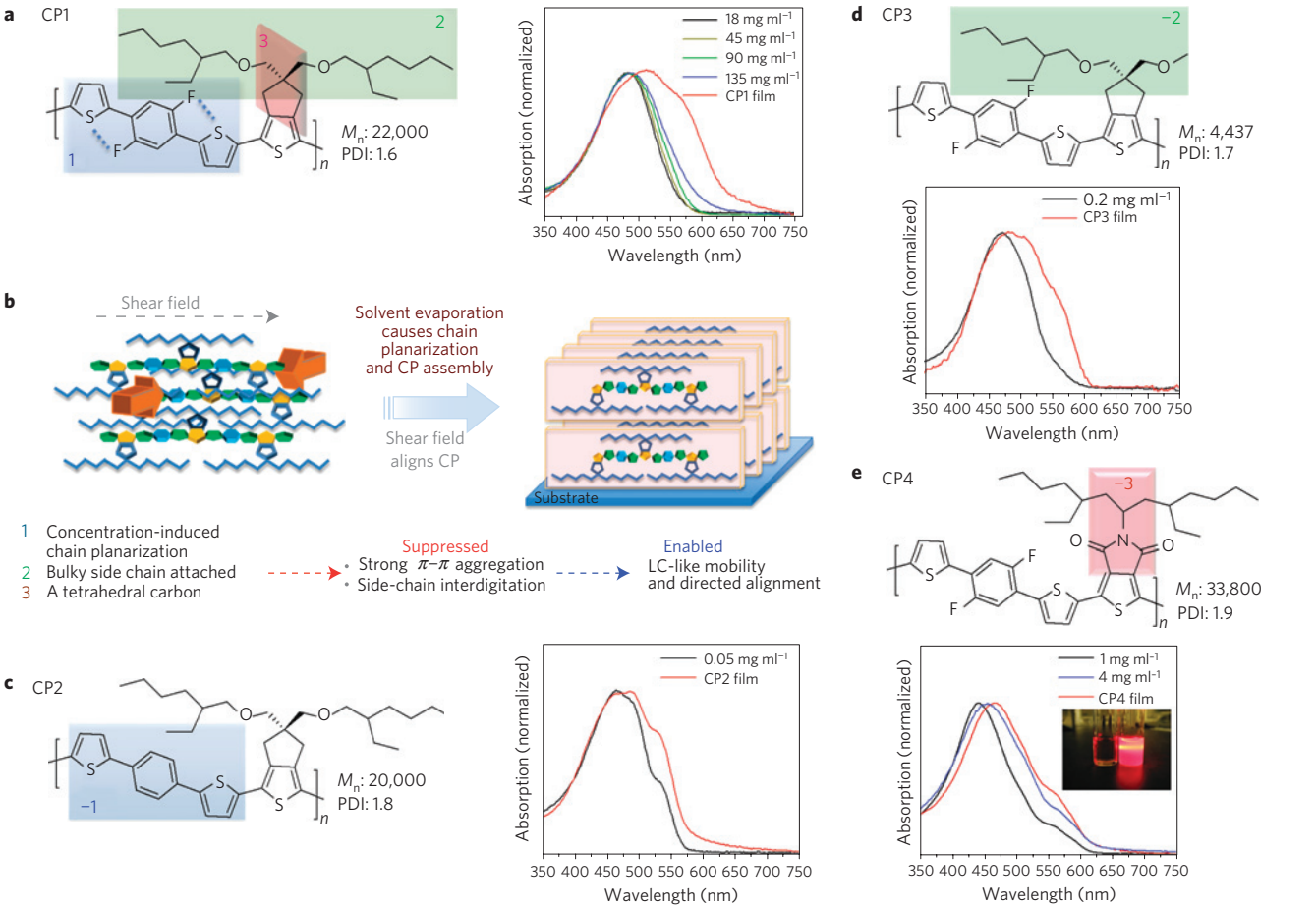

Figure 1 | The chemical structures of the designed CPs, their absorption spectra (in solution and as films) and the suggested mechanism for directed CP alignment. a, CP1 possesses three requirements for alignment under small shear flow. **b**, The suggested mechanism demands chain planarization under regulated aggregation. **c**, CP2 is an example of absent planarization. **d**, Massive interdigitation in CP3 frustrates chain freedom for alignment. **e**, Strong aromatic face-to-face interactions hinder CP4's response to applied shear flow. LC, liquid crystal.

use CPs' anisotropic electronic and optical properties, a molecular design principle of CPs combined with an efficient directed aligning strategy should be devised so that aligned thin conducting CPs layers and lines can be fabricated directly on a substrate.

Here, we systematically investigated and established a molecular design principle of CPs to achieve directed alignment of CPs along an applied flow field and achieved a high dichroic ratio of 16.67 in emission and 9.8 in absorption from well-aligned conducting CP thin films. Also, the anisotropic optoelectronic properties of these specific CPs in field-effect transistors (FETs) was realized. As shown in Fig. 1, four different CPs sharing the same chemical backbone were synthesized. We indicate the three important design features on the chemical structure of CP1 in the figure as: concentration-induced chain planarization, a carbon atom with tetrahedral out-of-plane bonding, and bulky side chains preventing side-chain interdigitation. The difference between CP1 and CP2 is the two fluorine (F) atoms on the benzene moiety in CP1, which was designed to investigate the influence of the S–F interaction on the intramolecular geometry and ultimately as a means to regulate chain planarity (Fig. 1c). The interaction between S and F atoms has been reported to improve carrier mobility because it is strong enough to enhance the crystallinity of small molecules[23,24]. To minimize intermolecular S–F interaction and massive polymer aggregation induced by strong intermolecular π–π interactions, two bulky 2-ethylhexyl side chains were introduced at the tetrahedral position of the second repeat unit (Fig. 1a). The second repeat unit having this unique structural form factor provides a liquid-crystalline property to CP1 by not only preventing the polymer from massive aggregation and but also inhibiting side-chain interdigitation (liquid-crystal images in Supplementary Fig. S1). To investigate the role of the bulky side chains and the necessity of the tetrahedral carbon having out-of-plane bonds, a third CP (CP3) and a fourth CP (CP4) were designed and synthesized, respectively. CP3 has the same chemical structure as CP1 except it has only one 2-ethylhexyl side chain rather than two side chains (Fig. 1d). We kept the same two bulky 2-ethylhexyl side chains when we designed CP4 but substituted the tetrahedral carbon linkage with two out-of-plane bonds for a nitrogen linkage with one in-plane bond (Fig. 1e). The new CPs were synthesized by using Suzuki or Stille type reactions with Pd(0) catalysts. The detailed synthetic procedures are described in Supplementary Scheme S1 and Scheme S2. The resulting CPs have very similar absorption spectra in solution (Fig. 1) because of their structural similarity. When the chain conformations of the CPs were quantum mechanically calculated by time-dependent density functional theory, the four CPs exhibited analogous chain geometries with similar twist angles between each monomer as illustrated in Supplementary Fig. S2, which explains their similar absorption behaviour in solution.

When a solution of CP1 in *o*-dichlorobenzene (10 mg in 4 ml) was drop-cast on a hydrophilic substrate on a hot plate, such as glass, indium tin oxide and polyvinyl alcohol film, a flow field was formed as the solvent evaporated during thermal treatment. The spontaneous flow field of CP1 could be attributed to its low

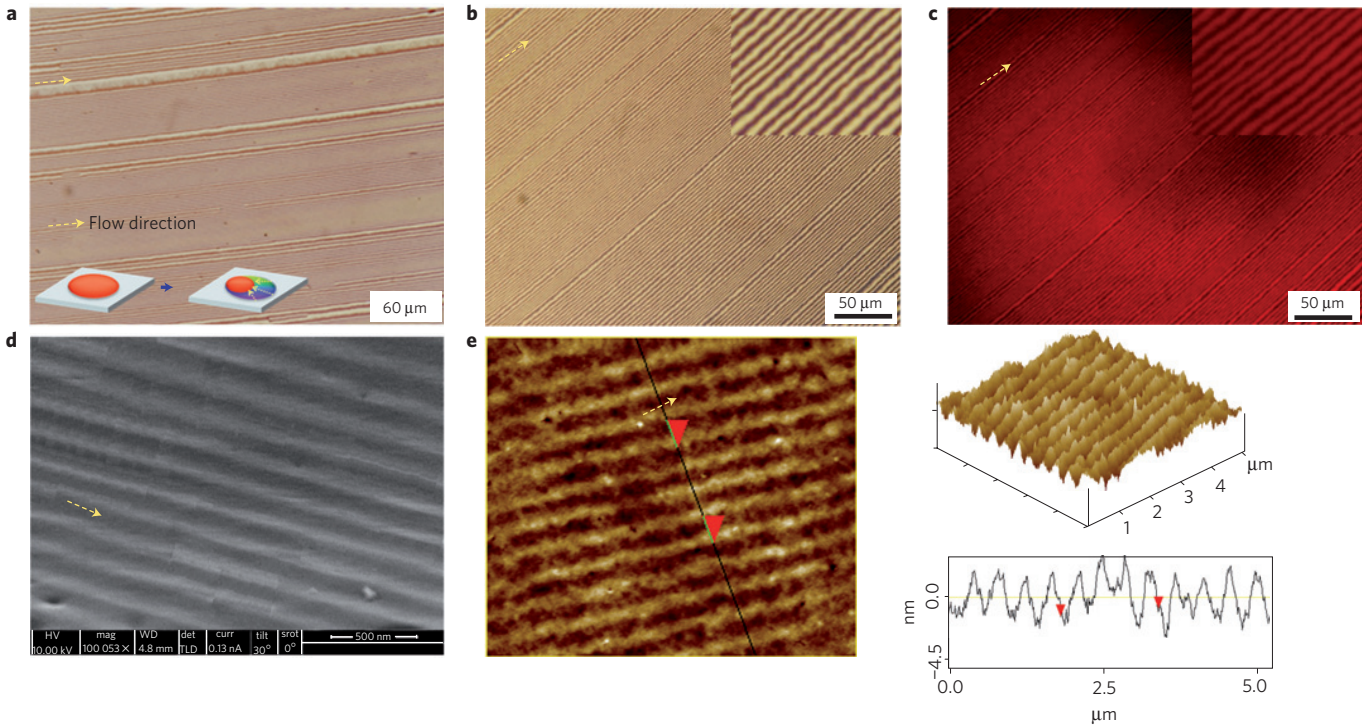

Figure 2 | The grooves generated from the flow of CP1 solution and their morphology analysis. a, Optical micrograph of the groove obtained without additive. The inset schematically illustrates the self-alignment phenomenon as the solvent evaporates from the drop-cast film. **b**, Optical micrograph of the groove obtained with additive, which indicates that a non-volatile additive is helpful for the groove generation mechanism. **c**, The grooves exhibited a bright and dark emission along their directions. The insets of **b**,**c** are magnified grooves (the horizontal length of the inset is 35 μm). **d**, SEM image of the grooves. **e**, AFM image of the grooves and the section analysis on the right side reveal that the generated grooves have a regular feature of 5 nm in amplitude and of 200–300 nm in periodicity.

surface energy originating from the F atoms as confirmed with a water contact angle of 101.5°. Interestingly, the flow of CP1 solution produced unidirectional grooves (Fig. 2a), which have the same direction as the flow. Adding an additive (5 vol%, 1,8-diiodooctane or octanedithiol) to the CP1 solution improved the uniformity of the resulting grooves as shown in Fig. 2b, indicating that the non-volatile additive is helpful for the groove generation mechanism in the CP1 film. The grooves exhibited a bright and dark reddish emission along their direction (Fig. 2c). Even though the Marangoni effect caused by the surface tension difference during solvent evaporation is probably responsible for the groove formation, we do not fully understand the groove forming mechanism yet. High-resolution scanning electron microscopy (SEM; Fig. 2d) and tapping-mode atomic force microscopy (AFM; Fig. 2e) revealed that the grooves have regular features, exhibiting about 5 nm in amplitude and a 200–300 nm period. To analyse the nature of the grooves, the CP1 film was characterized by grazing-incidence X-ray diffraction (GIXRD) with a 2D detector because it provides both lateral and vertical order information for thin films. The 2D GIXRD measurement was carried out both parallel (Fig. 3a, in-groove) and perpendicular (Fig. 3b, out-groove) to the grooves in a single sample. In the case of y axis scattering, both in-groove and out-groove directions showed the same scattering pattern, corresponding to a lamella-like orientational order, with a similar scattering intensity. Only the in-groove direction, however, exhibited noticeable x-axis scattering (Fig. 3a), implying that the generated lamella have a principal positional order along the flow field direction. The X-ray diffractogram (Fig. 3c, converted from the 2D scattering images) revealed that the interchain distance ($2\theta = 4.3°$, 20.5 Å) was comparable to double the calculated side chain distance (10.5 Å) of the polymer backbone, as illustrated in Fig. 3d. We believe that the branched bulky side chains, two 2-ethylhexyl groups at the tetrahedral position, have minimized interchain interactions, which results in barely interdigitated CP1 chains. This turns out to be one of the key molecular design features to achieve directed alignment (see below). As shown in Supplementary Fig. S3, however, when a CP1 film was fabricated by spin-casting, we could see only an immature lamellar structure without any x-axis scattering, indicating a lack of inter-lamellar ordering; spin-casting dries the film rapidly and probably does not allow enough time or mobility for the polymer chains to be self-assembled and oriented.

Interestingly, CP2 without intramolecular S–F interaction capability did not show any alignment and generated only primary scattering corresponding to the interchain distance (Supplementary Fig. S3b). The reason for the distinguishable self-assembly behaviours between CP1 and CP2 can be traced to their different molecular geometry originating from the intramolecular S–F interaction. Initially, both CPs are fully solvated by a good solvent and have a similar conformation confirmed by their solution ultraviolet–visible spectra. During the solvent evaporation, the free volume occupied by solvent molecules decreases and the polymer chains reorient to minimize steric hindrance as they are forced to be closely packed. One common type of reorientation routes of CPs is their backbone rotation because of their inherently rigid rod-like framework[25]. This rotation triggers the intramolecular S–F interaction and produces planar segments in the CP1 backbone as illustrated in Fig. 1b. Then, the planar segments accelerate interchain assembly through π–π interaction. However, the bulky side chains attached to the tetrahedral position of the second repeat unit prevent massive aggregation, which gives a mobile crystalline-like nature to the CP1 chains, much like liquid crystals. The ultraviolet–visible spectra of CP1 in a solution and a solid film clearly support our explanation. As can be clearly seen, the

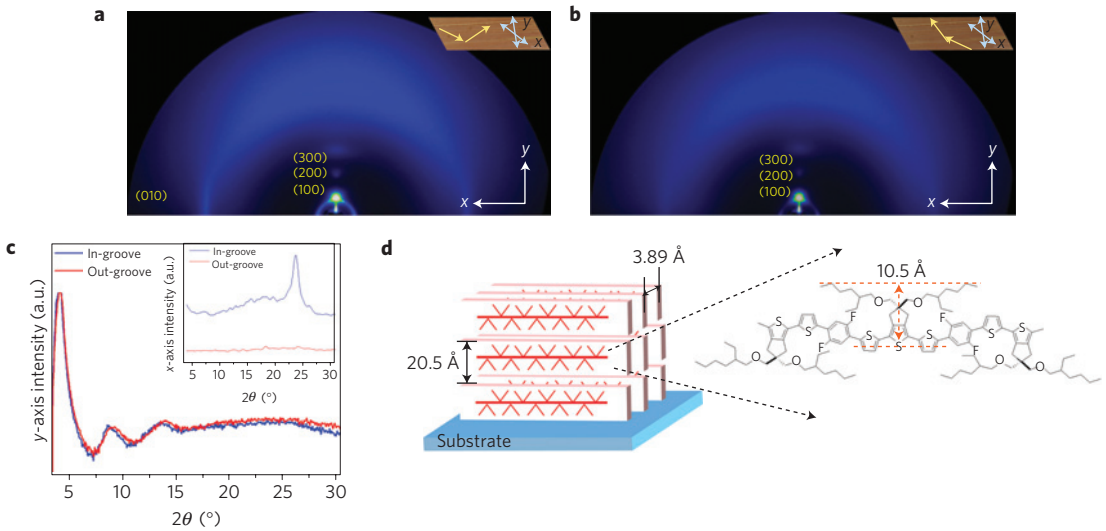

Figure 3 | GIXRD with CP1. a,**b**, GIXRD was carried out on the same CP1 film but under different incident directions: parallel (in-groove along the yellow arrows, **a**) and perpendicular (out-groove along the yellow arrows, **b**). **c**, 2D GIXRD images and the diffractogram converted from the images. **d**, A model developed on the basis of the GIXRD reveals that the grooves are from aligned lamella having comparable dimensions of individual CP1 chains. The horizontal red lines represent the polymer backbone and the attached chevrons are the 2-ethylhexyl side chains.

absorption of CP1 showed a large redshift in the solid film (Fig. 1a). Usually, a large redshift of the absorption λ_{max} from solution to a film state can be explained by strong intermolecular aggregation and/or increased effective conjugation due to chain planarization[25]. As the bulky 2-ethylhexyloxy side chains were introduced at the tetrahedral position to minimize intermolecular chain packing, the unique and large absorption change of CP1 in the solid film could be ascribed to the chain planarization through the intramolecular S–F interaction. Examining the absorption spectra of CP2 in a solution and a solid film verifies this claim. As shown in Fig. 1c, CP2 without the S–F interaction capability showed only a minimal redshift from the solution to the solid film.

To investigate the importance of the non-interdigitated side-chain packing of CP1 for the directed alignment capability, we synthesized CP3 that comprised only one 2-ethylhexyl side chain. X-ray diffraction data showed an interchain distance of 1.65 nm, which is much smaller than that of CP1 (2.10 nm), indicating the interdigitated nature of the side chains of CP3 (Supplementary Fig. S3c). CP3 indeed did not show the alignment phenomenon. We believe that the interdigitated side chains interlock the CP3 chains along the film thickness direction, reduce the chain mobility and the aspect ratio, and consequently prevent the rod-like individual CP3 chain from aligning, whereas the non-interdigitated bulky side chains of CP1 endow liquid-like mobility to CP1 so that it can align along the shear direction.

Is the tetrahedral carbon linker characterized by the two out-of-plane bonds or an analogous moiety with a large form factor necessary to realize the directed alignment feature through preventing a strong π–π interchain interaction of CPs? We synthesized CP4 with the same two 2-ethylhexyl side chains but connected to a nitrogen linker rather than a tetrahedral carbon linker. X-ray diffraction analysis on CP4 films showed an interchain distance of 2.81 nm, implying non-interdigitated side chains like CP1 (Supplementary Fig. S3c). However, we could not observe any alignment feature from CP4. We investigated the aggregation behaviour of CP4 compared with CP1 to understand the importance of the tetrahedral carbon linker. We prepared solutions of CP1 and CP4 in *o*-dichlorobenzene at various concentrations and recorded the absorption spectra of each solution (Fig. 1). Whereas CP1 did not show any significant redshift even at a very high concentration of 135 mg ml^{-1}, CP4 exhibited aggregation and particle formation at a concentration of only 4 mg ml^{-1}. As shown in the inset of Fig. 1e, the 4 mg ml^{-1} solution of CP4 exhibited the Tyndall effect due to the particle formation. Therefore, we conclude that CP4, without a tetrahedral carbon, aggregates well. The aggregates do not have a large enough aspect ratio nor good enough mobility to be aligned along the flow field. The structural analysis, optical properties and alignment behaviour of the designed four CPs consistently support our molecular design principle for efficient polymer alignment.

To direct the alignment direction of the CP1 chains, we applied a contact coating system that can adjust both the coating speed and the thickness of the film (Supplementary Fig. S4). As shown in Fig. 4a, we obtained a well-aligned CP1 film along the applied contact coating direction. In this system, the blade maintained contact with the CP1 solution through capillary force. As the coating speed decreases, more narrow and homogeneous grooves were produced (Supplementary Fig. S5a–d). The width of the coating area under an optimized coating condition (speed; 25 μm s^{-1}, gap; 50 μm) was over 20 mm. To quantify the alignment of CP1 realized by the contact coating method, the emission intensities of the film were investigated using a linear polarizer. As depicted in Fig. 4b, the emission intensity decreased as the direction of the polarizer deviated from parallel to perpendicular to the contact coating direction, indicating a parallel alignment of CP1 along the coating direction. Interestingly, as the coating speed decreased, a higher degree of polymer alignment was achieved judging from the dichroic ratio in emission (the emission intensity parallel to the alignment direction/the emission intensity perpendicular to the alignment direction; Supplementary Fig. S5). Whereas the film obtained with a 100 μm s^{-1} coating speed exhibited a dichroic ratio of 4.76, the film produced with a 25 μm s^{-1} coating speed produced a much larger dichroic ratio of 16.67. This is counterintuitive because a faster coating speed should produce a larger flow field and thus better chain alignment. The reason for this counterintuitive phenomenon can be found from the CP1 design for directed alignment. Until sufficient solvent evaporates, CP1 will not have a planar conformation and in this state the polymer chain cannot be effectively aligned owing to the small size of the individual chain (see above); the same reason that the non-volatile additive improved the polymer alignment. Therefore, a slower coating speed will allow more solvent evaporation and induce more effective chain

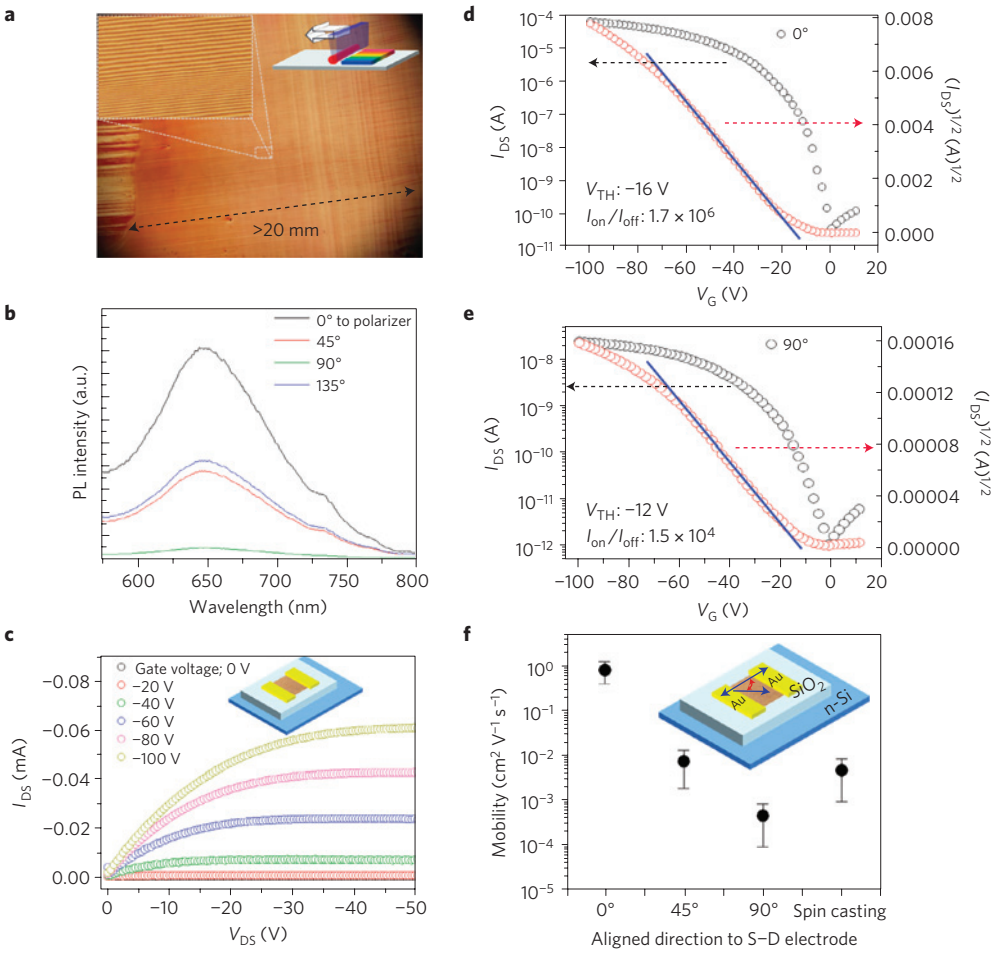

Figure 4 | Directed alignment and its optical/electrical anisotropic properties. a, Optical micrograph of an aligned CP1 film by the contact coating method illustrated in the inset. The inset shows parallel grooves. **b**, Emission intensity of an aligned CP1 film through a linear polarizer oriented with a different angle to the CP1 alignment direction. 0° means parallel orientation, and 90° means perpendicular orientation. **c**, Output curve of a FET device built on the aligned CP1 film. The source–drain direction is parallel to the CP1 alignment direction. **d**, Transfer curve of a FET device with a source–drain oriented parallel to the CP1 alignment direction. **e**, Transfer curve of a FET device having a source–drain oriented perpendicular to the CP1 alignment direction. **f**, Hole mobility of FET devices depending on the orientation of the source–drain relative to the CP1 alignment direction. Compared with the perpendicular direction, the chain alignment direction had a faster hole mobility by more than three orders of magnitude. The insets show the geometry of the device and the orientation of the electrodes relative to the alignment direction of CP1. The double-headed blue arrow is the source–drain direction. The single-headed blue arrow represents the CP1 alignment direction. The angle between the two arrows (0°, 45° and 90°) is the aligned direction to the source–drain electrode.

planarization and self-assembly. The self-assembled liquid like CP1 will then align along the flow field.

The molecular weight of the CPs also influences the degree of alignment. We obtained a larger dichroic ratio as the molecular weight of CP1 increased (Supplementary Fig. S5e). The enlarged molecular weight would endow a higher aspect ratio to the rigid frame, resulting in better intermolecular assembly as similarly described in a previous report[26]. As shown in Supplementary Fig. S5e–g, the maximum dichroic ratio could be obtained at 140 °C on a glass substrate when CP1 (M_n: 22,000) solution was applied at a coating speed of 25 μm s^{-1}. As the fabrication temperature approaches the boiling point of the applied solvent (*o*-dichlorobenzene, 180 °C), the distribution of the dichroic ratio becomes wide probably because the translational motion of CP/solvent hampers chain orientation to the applied shear direction. CP1 could also be aligned on polymeric substrates such as polyvinyl alcohol but the degree of alignment was poorer than that on inorganic substrates probably owing to the larger surface roughness of the polymer substrates or the enhanced interaction between the CP1 solution and the polymer substrates.

We applied the same contact coating method to CP2, CP3 and CP4. None of these CPs showed any alignment as shown in Supplementary Fig. S5e. Basically, the dichroic ratio of CP2 to CP4 is 1, indicating their random orientation. Compared with CP 1, CP2 and CP4, the molecular weight of CP3 (M_n = 4,437) is much smaller and a CP with a smaller molecular weight is prone to have worse orientation along the shear direction as a consequence of its reduced aspect ratio, as Supplementary Fig. S5e demonstrates. However, the random orientation of CP3 is probably not due to its small molecular weight because CP1, having a comparable molecular weight (M_n = 6,500), showed a dichroic ratio of 9.2±1.8 at a coating speed of 25 μm s^{-1}. The degree of polymerization of CP1 is 9.5, which is comparable to that of CP3 (7.6).

We built FET devices with a top-contact and bottom-gate configuration on the well-aligned CP1 film to demonstrate how the anisotropic properties of CPs can be realized in a device application. A heavily doped *n*-type Si/SiO_2 wafer was used as the substrate, wherein the conductive Si wafer and the surface SiO_2 layer (~260 nm) function as the common gate electrode and the gate dielectric, respectively. As shown in the output and transfer curves (Fig. 4c,d) of a FET device having the same

source–drain (S–D) direction to the alignment, the hole mobility ($\mu(0°)$) extracted from the saturation regime is 0.86 $cm^2\ V^{-1}\ s^{-1}$, with a current on-to-off ratio (I_{on}/I_{off}) of 1.7×10^6 and a threshold voltage (V_{TH}) of around −16 V. The FET carrier mobility sensitively changed depending on the S–D direction relative to the polymer alignment direction (Fig. 4d–f and Supplementary Fig. S6). The fastest hole mobility was obtained along the polymer alignment direction ($\mu(0°) = 0.86\ cm^2\ V^{-1}\ s^{-1}$), which was more than 3 orders of magnitude higher than the slowest hole mobility extracted from the perpendicular direction to the polymer alignment, $\mu(90°)$ of 0.00054 $cm^2\ V^{-1}\ s^{-1}$. This result clearly indicates that the intrachain carrier transfer along conjugated polymer backbones is much more efficient when compared with the interchain charge hopping through π–π stacks, even though the hopping rate could be different depending on the intermolecular distance[27,28]. The hole mobility of spin-cast films, which is comparable to the immaturely assembled state of the CP1 film as demonstrated in Supplementary Fig. S3, exhibited a slightly smaller value than that of the midway direction ($\mu(45°)$) of the alignment direction. This was still about 1–2 orders of magnitude faster than the transverse mobility ($\mu(90°)$).

We have developed a CP design principle to achieve directed CP assembly and alignment. Three important molecular design components are identified: concentration-induced chain planarization, a tetrahedral carbon linker with out-of-plane bonding, and bulky side chains preventing side-chain intercalation. When a CP satisfied these three design requirements, the rigid rod-like CP chains could be aligned when they were exposed to a shear flow/force. By applying a contact coating method, the alignment direction could be directed and the degree of alignment was optimized by means of the coating speed. The very high dichroic ratio of 16.67 in emission was achieved by this method. FET devices built on the aligned CP1 film showed more than three orders of magnitude faster hole mobility along the chain alignment than perpendicular to the alignment direction. The presented molecular design principle for directed alignment of CPs is readily applicable to many CP developments for various optoelectronic applications and to achieve the full realization of the anisotropic properties of CPs in device applications. The strategic combination of the developed lyotropic liquid-crystalline CP design rules, rationally devised chemical structures of CPs for an intrinsic intramolecular high hole mobility, and a new fabrication scheme, may open the door to wet-processable high-performance plastic electronics.

Received 11 June 2012; accepted 5 February 2013; published online 24 March 2013

References

1. Kim, Y. *et al.* A strong regioregularity effect in self-organizing conjugated polymer films and high-efficiency polythiophene:fullerene solar cells. *Nature Mater.* **5,** 197–203 (2006).
2. Chen, H-Y. *et al.* Polymer solar cells with enhanced open-circuit voltage and efficiency. *Nature Photon.* **3,** 649–653 (2009).
3. Park, S. H. *et al.* Bulk heterojunction solar cells with internal quantum efficiency approaching 100%. *Nature Photon.* **3,** 297–303 (2009).
4. McCulloch, I. *et al.* Liquid-crystalline semiconducting polymers with high charge-carrier mobility. *Nature Mater.* **5,** 328–333 (2006).
5. Sirringhaus, H. *et al.* Two-dimensional charge transport in self-organized, high-mobility conjugated polymers. *Nature* **401,** 685–688 (1999).
6. Ha, J. S., Kim, K. H. & Choi, D. H. 2,5-Bis(2-octyldodecyl)pyrrolo[3,4-c]pyrrole-1,4-(2H,5H)-dione-based donor–acceptor alternating copolymer bearing 5,5′-di(thiophen-2-yl)-2,2′-biselenophene exhibiting 1.5 $cm^2\ V^{-1}\ s^{-1}$ hole mobility in thin-film transistors. *J. Am. Chem. Soc.* **133,** 10364–10367 (2011).
7. Gross, M. *et al.* Improving the performance of doped p-conjugated polymers for use in organic light-emitting diodes. *Nature* **405,** 661–665 (2000).
8. Lavastre, O., Illitchev, I., Jegou, G. & Dixneuf, P. H. Discovery of new fluorescent materials from fast synthesis and screening of conjugated polymers. *J. Am. Chem. Soc.* **124,** 5278–5279 (2002).
9. Thomas, S. W. III, Joly, G. D. & Swager, T. M. Chemical sensors based on amplifying fluorescent conjugated polymers. *Chem. Rev.* **107,** 1339–1386 (2007).
10. Forzani, E. S. *et al.* A conducting polymer nanojunction sensor for glucose detection. *Nano Lett.* **4,** 1785–1788 (2004).
11. Gibbons, W. M., Shannon, P. J., Sun, S-T. & Swetlin, B. J. Surface-mediated alignment of nematic liquid crystals with polarized laser light. *Nature* **351,** 49–50 (1991).
12. Grell, M. *et al.* A glass-forming conjugated main-chain liquid crystal polymer for polarized electroluminescence application. *Adv. Mater.* **9,** 798–802 (1997).
13. Grell, M. *et al.* A. Blue polarized electroluminescence from a liquid crystalline polyfluorene. *Adv. Mater.* **11,** 671–675 (1999).
14. Lee, J., Jun, H. & Kim, J. Polydiacetylene–liposome microarrays for selective and sensitive mercury(II) detection. *Adv. Mater.* **21,** 3674–3677 (2009).
15. Brinkmann, M & Wittmann, J-C. Orientation of regioregular poly(3-hexylthiophene) by directional solidification: A simple method to reveal the semicrystalline structure of a conjugated polymer. *Adv. Mater.* **18,** 860–863 (2006).
16. Cremer, L. D., Verbiest, T. & Koeckelberghs, G. Influence of the substituent on the chiroptical properties of poly(thieno[3,2-b]thiophene)s. *Macromolecules* **41,** 568–578 (2008).
17. Cimrová, V., Remmers, M., Neher, D. & Wegner, G. Polarized light emission from LEDs prepared by the Langmuir–Blodgett technique. *Adv. Mater.* **8,** 146–149 (1996).
18. Kim, J., McHugh, S. K. & Swager, T. M. Nanoscale fibrils and grids: Aggregated structures from rigid-rod conjugated polymers. *Macromolecules* **32,** 1500–1507 (1999).
19. Weder, C., Sarwa, C., Montali, A., Bastiaansen, C. & Smith, P. Incorporation of photoluminescent polarizers into liquid crystal displays. *Science* **279,** 835–837 (1998).
20. Montali, A., Bastiaansen, C., Smith, P. & Weder, C. Polarizing energy transfer in photoluminescentmaterials for display applications. *Nature* **392,** 261–264 (1998).
21. Tsao, H. N. *et al.* The influence of morphology on high-performance polymer field-effect transistors. *Adv. Mater.* **21,** 209–212 (2009).
22. Zheng, Z. *et al.* Uniaxial alignment of liquid-crystalline conjugated polymers by nanoconfinement. *Nano Lett.* **7,** 987–992 (2007).
23. Subramanian, S. *et al.* Chromophore fluorination enhances crystallization and stability of soluble anthradithiophene semiconductors. *J. Am. Chem. Soc.* **130,** 2706–2707 (2008).
24. Gundlach, D. J. *et al.* Contact-induced crystallinity for high-performance soluble acene-based transistors and circuits. *Nature Mater.* **7,** 216–221 (2008).
25. Kim, J. & Swager, T. M. Control of conformational and interpolymer effects in conjugated polymers. *Nature* **411,** 1030–1034 (2001).
26. Tsao, H. N. *et al.* Ultrahigh mobility in polymer field-effect transistors by design. *J. Am. Chem. Soc.* **133,** 2605–2612 (2011).
27. Lemaur, V. *et al.* Charge transport properties in discotic liquid crystals: A quantum-chemical insight into structure-property relationships. *J. Am. Chem. Soc.* **126,** 3271–3279 (2004).
28. Yuen, J. D. *et al.* Nonlinear transport in semiconducting polymers at high carrier densities. *Nature Mater.* **8,** 572–575 (2009).

Acknowledgements

The authors thank E-H. Sohn at Seoul National University (SNU) for the 2D GIXRD measurement and J. Kieffer and X. Ma for the calculation of the polymer conformation. This work was supported by the US Department of Energy (DOE), Office of Basic Energy Sciences, as part of the Center for Solar and Thermal Energy Conversion, an Energy Frontier Research Center (DE-SC0000957). E.J.J. was partly supported by the WCU (World Class University) programme through the National Research Foundation of Korea funded by the Ministry of Education, Science and Technology (R31-2008-000-10075-0) and S.S. was supported by an NSF CAREER Award (DMR 0644864).

Author contributions

J.K. designed and directed the project. B-G.K. and E.J.J. synthesized the series of polymers. B-G.K. prepared and analysed the aligned CP films, B-G.K., J.W.C. and B.K. fabricated the organic thin-film transistors, and S.S. performed the X-ray measurements. B-G.K. and J.K. wrote the manuscript, and all other authors had input.

Additional information

Supplementary information is available in the online version of the paper. Reprints and permissions information is available online at www.nature.com/reprints. Correspondence and requests for materials should be addressed to J.K.

Competing financial interests

The authors declare no competing financial interests.